FIRST SIR-C SCANSAR RESULTS

C.Y. Chang, Michael .Y. Jin, Yun-Ling Lou, Benjamin Holt
Jet Propulsion laboratory
California Institute of Technology
M/S 300-235
4800 Oak Grove Drive
Pasadena, Ca 91109

ABSTRACT

During the two very successful space shuttle missions in 1994, in addition to acquiring a large volume of' data using the continuous strip mode, the Spaceborne Imaging Radar-C (SIR-C) also acquired several experimental datatakes using the ScanSAR mode. ScanSAR was made possible by SIR-C'S phase array antenna. During the ScanSAR operations, the antenna beam was swiftly steered from one look angle to another to step through the entire swath. Some of these Scan SAR data have been processed into images of swaths wider than 200 kilometers. These early results demonstrate that ScanSAR operation is not only feasible but also represents a powerful tool for regional and global scale imaging by the future SAR missions.

I. INTRODUCTION

Since the Synthetic Aperture Radar (SAR) was first employed by the SEASAT mission for remote sensing applications, most civilian SAR systems developed so far have been operated in the continuous strip mode [1]-[2]. For such a radar mode, the antenna beam is pointed to the broadside, at near right angles to the flight track, and the radar is continuously pulsing and receiving the returned echoes. This enables production of either single-look imagery of full azimuth resolution or multi-look imagery of slightly lower azimuth resolution. The data rate of the radar system is limited either by the downlink channel or by the flight recorder. A wider swath is often achieved by reducing the number of bits per raw data sample, by employing raw data compression schemes, or by reducing the pulse bandwidth. The first two options trade the dynamic range for a wider swath. The third option trades the range resolution for a wider swath.

Another radar mode known as the burst mode was employed by the Magellan mission which mapped the surface of the Venus [3]. For the burst mode, the radar transmits pulses in bursts (or groups) according to the commanded burst length and duty cycle. As a result of the burst operation, only partial azimuth phase history (partial bandwidth) is recorded, which degrades the azimuth resolution. Overall, the burst mode operation trades the azimuth resolution for a lower data rate or less power consumption.

The ScanSAR mode can be viewed as an extension of the burst mode [4]-[5]. For instance, the four-beam ScanSAR transmits a number of pulses at look angle one, some pulses at look angle two, and some more pulses at look angle three and four, after that the antenna beam is steered back to look angle one and the same procedure continues as depicted in Figure 1. The same concept applies to any other multi-beam ScanSAR modes. ScanSAR data is thus composed of multiple subswaths where each subswath data is acquired in a way similar to the burst mode. Compared to the continuous mode, the ScanSAR mode trades the azimuth resolution for a wider swath.

The Spaceborne imaging Radar-C (SIR-C), the third in a series of space shuttle based synthetic aperture radars (SAR) sponsored by the National Aeronautics and Space Administration (NASA), was flown twice aboard space shuttle Endeavour in 1994: the first one in April and the second one in October [G]. Silt-C operates at L- and C-band frequency with quad-polarization capability. More than one hundred hours of science data were acquired from the two eleven-day space shuttle missions. During both space shuttle missions, the radar

was occasionally commanded to operate in several experimental modes: ScanSAR, spotlight and squint mode. ScanSAR data were acquired over four SIR-C sites: Prince Albert in Saskatchewan, Canada; Chickasha in Oklahoma, United States; North Atlantic Ocean; and Weddell Sea, Antarctica. ScanSAR data were transferred and processed by the modified SIR-C survey processor into subswath images which were later mosaicked to form the full-swath imagery. Some data were also used to test out the RADARSAT Scan SAR processor that is being developed at the Jet Propulsion laboratory (J I 'L) for implementation at the Alaska SAR Facility (ASF). ASF is a NASA-sponsored Distributed Active Archive Center (DAAC) operated by the University of Alaska, Fairbanks. An example SIR-C Scan SAR data set was generated and made available for several processing facilities around the world. Many of these processing facilities arc developing systems for processing the upcoming RADARSAT data.

RADARSAT, the first spaceborne SAR system sponsor cd by Canada, is scheduled for launch on a Delta II rocket from Vandenberg Air Force Base in October, 1995 [7]. RADARSAT is capable of operating in both continuous mode and ScanSAR mode. It will become the first spaceborne SAR system operationally acquiring ScanSAR data for monitoring earth surfaces at regional and global scales.

This paper presents the first results on SIR-C ScanSAR images. Section II describes the SIR-C ScanSAR data acquisition scenario. Section 111 reviews the ScanSAR processing algorithm. Section IV presents SIR-C ScanSAR images. Additional applications of ScanSAR by the future SAR missions arc addressed in the end of the paper.

II. SIR-C SCANSAR DATA ACQUISITION

The SIR-C flight system consists of an antenna structure and RF electronics integrated into the Shuttle payload bay and digital electronics and high rate recorders located in the crew cabin. The SIR-C radar system employs a planar active phase array antenna. The antenna beam can be electronically steered over a $\pm 23°$ range in elevation and over a $\pm 2°$ range in azimuth. The antenna panel was mounted into the payload bay with a 14° mechanical tilt angle and the space shuttle nominally flew with a 26° roll angle, which resulted in a 40° off-nadir look angle without any electronic steering. Key orbit and radar characteristics arc summarized in Table 1. More detailed description of t he SIR-C flight system can be found in [8].

The SIR-C radar system was commanded to operate in a number of] adar modes with various frequency band and polarization channel combinations. Received echoes were digitized at a rate of 180 Megabits per second. Digitized data were recorded on high density digital cassettes and further processed by the ground data pi ocessing system. Numerous products have been and arc being produced for analysis by the Silt-C science team as well as for distribution to the general public.

During the two eleven-day space shuttle missions, most of the science data were acquired using the continuous strip mode. Additionally, a fcw number of experimental datatakes were acquired using Scan SAR, spotlight and squint mode, l'able 2 summarizes the ScanSAR datatakes from both flights, which total up to about onc hour worth of data.

To illustrate how radar parameters were set up, Table 3 shows the commanded radar parameters for flight 2 datatake 82.1. This datatake was acquired during an ascending pass over Chickasha in Oklahoma on Day 5 of the second mission for a duration of 3 minutes and 24 seconds. It used the four-beam Scan SAR mode. Electronic steering angles for these four beams were commanded to be –1 O.O°, 0.5°, 7.25° and 11.00, which translate into 30.0°, 40.5°, 47.25° and 51.00 off-nadir look angles, respectively, when taking into account the nominal shuttle roll of 26° from nadir and a mechanical tilt of 14°. Both I,-band and C-band radars transmitted V-polarization pulses simultaneously and returned echoes were recorded by 11- and V-polarization receivers. This produces four channels of data: LVV, LVH, CVV and CVH. The PRF value was chosen independently from the near-range to the far-range beam for reducing the ambiguity, transmitter and nadir interference effects. The 10 MHz pulse band width was used, resulting in a 15-meter slant range resolution. The dwell time of a beam was usually selected so that it gradually increased as a function of look angles to maintain similar azimuth resolutions. L- and C-band data were acquired using the same dwell time. As a result, the L-band one-look azimuth resolution is approximately four times as large as the C-band. The minimum dwell time is constrained to be 30 mini-seconds by the flight system timing. For the four-beam ScanSAR mode, this results in a C-band image with slightly more than onc look before any pixel aver aging is applied.

III. SCANSAR PROCESSING ALGORITHM

in order to attain a high throughput rate, the burst mode and the ScanSAR mode data arc often pi ocessed by the spectral analysis (SPECAN) algorithm [9]. Following range compres-

sion, the SPECAN algorithm first removes the quadratic phase components from the azimuth phase history. After that, the remaining linear phase terms are only dependent upon targets' along-track positions relative to the center of the burst, which allows targets to be separated by the Fourier transformation. Detailed description and analysis of the SPECAN algorithm can be found in [9].

As a result of the burst mode operation, the intensity of the burst image is modulated by the azimuth antenna pattern. This special feature is known to be the scalloping effect. Following azimuth compression, radiometric correction is required to compen sate for this along-track radiometric modulation. The SPECAN algorithm also results in an image represented in the so-called range-l)opplcr domain where the two axes are curved iso-range and iso-Doppler lines. This phenomenon is known to be the fanshape effect,. Geometric rectification is required to resample the slant range-I)opplcr images into a rectangular grid before images are overlaid together to form the multi-look in ıagery.

For ScanSAR processing, additional steps are required to mosaic subswath images into the final full-swath imagery. Line offsets are determined by the elapsed time from onc burst of a beam to another burst of the immediate beam. Pixel offsets are controlled by the differences in the slant ranges to the first raw data samples. Determination of pixel locations and selection of the projection model are critical to producing a seamless ScanSAR image. Figure 2 summarizes the flow diagram for processing ScanSAR data.

IV. SIR-C SCANSAR RESULTS

Figure 3 shows an example SIR-C ScanSAR image. It was processed from the first 40 seconds of flight 2 datatake 82.1. Key radar parameters are summarized in Table 3. This data segment was acquired over western Texas. It is an 1,-band VV-polarization image. The swath width is 225 Km and the image size in the along-track direction is 270 Km. The ground resolution is approximate] y 100 m. Range and azimuth antenna pattern modulation is effect i vc1 y removed from the image. Subswath images are perfectly overlaid in forming the full-swath image. This portion of western Texas is sparsely populated, with the largest cities of Midland and Odessa on the right hand side. The area contains extensive oil fields that surround nearly all the towns and cities, with the oil field equipment appearing as isolated bright point targets. Agricultural fields are also present. The town of Hobbs in the uppermost right corner of the image is located within New Mexico. The mountains near the

left hand portion of the image are the northern edge of the Sierra Madre Oriental mountain range that extends into Mexico. King Mountain at lower center is actually a flat mesa over 3,000 feet, high. The linear features nearing Hobbs are separated by intermittent stream beds.

For comparison, a standard SIR-C standard image, with a dimension of 100 Km in along-track and 57 Km in cross-track, is overlaid in the lower left corner of the ScanSAR image. This standard Silt-C image was processed from flight 1 datatake 82.1. This comparison clearly demonstrates the power of using ScanSAR for large scale imaging.

The radiometric quality of ScanSAR images is determined by several factors. These factors include signal-to-noise ratio (SNR), equivalent numbe of looks, and accuracy in estimating antenna pointing. For SIR-C, SNR is typically greater than 20 dB. The contribution by the noise floor to radiometric modulation is nearly negligible. 10J a ScanSAR system with a low SNR, the variation of the noise floor in the fin al image is expected to be relatively severe among subswaths. This variation is even intensified for a system which does not have sufficient number of looks, which is fairly common for a C-band system. This variation caused by the noise floor must be equalized during the data processing. When the antenna beam is steered from one look angle to another, the footprint of the antenna beam often exhibits a different curve from one to another duc to slightly different pointing angles. In order to reduce radiometric modulation effects, the processor must be capable of accurately estimating and tracking the antenna pointing angles across different beams. This is easier to do for the I.-band case as it has a wider antenna azimuth beamwidth. For a C-band ScanSAR system such as RADARSAT and the Sill-C C-band radar, the pointing accuracy is required to be four times better than the L-band. All these discussions show that it is more challenging to processiiig C-band ScanSAR data.

Figure **4** shows a color composite ScanSAR image of SIR-C. It was processed from the first 50 seconds of flight 2 datatake 87.7. Key radar parameters arc summarized in '1'able 4. The colors in this image were obtained using the following radar channels: L-band vertical transmit-vertical receive (VV) is blue, L-band horizontal transmit-vertical receive (HV) is green, and C-band VV is red. This radar image shows two large ocean circulation features called eddies at the northernmost edge of the sca icc pack of the Weddell Sea, off Antarctica. The eddy processes in this region play an important role in the circulation of the global ocean and the transportation of heat toward the pole. 'l'his is the first wide-swath multi-frequency, multi-polarization radar image ever processed. The image is oriented approximately east-

west, with a center location of around 56.6 degrees South and 6.5 degrees West. Image dimensions are 240 kilometers by 350 kilometers (149 miles by 218 miles) and the pixel size is 100 meters. The ocean eddies have a clockwise (or cyclonic) rotation and are roughly 40 to 60 km (25 to 37 miles) in diameter. Small sea-ice floes that are swept along by surface currents, are shown both within the eddies and to the south of the eddies in this image. Several distinct forms of sea ice are visible including grease ice (a slushy viscous form of new ice) which appears smooth and dark on the radar image; pancake ice, typically small, 1 to 2 meter (3 to 7 feet) diameter rounded ice floes formed by the clumping of grease ice under waves, which appears bright in the radar image and filamentous (lighter green); and first-year, seasonal ice, typically 0.5 to 0.8 meter (1.5 to 2.5 feet) thick, seen in the lower right corner as darker green color. The open ocean to the north is uniformly bright due to high winds making the surface rough.

V. FUTURE APPLICATIONS OF SCANSAR

SIR-C ScanSAR results demonstrate that ScanSAR operation is achievable by the current state- of-the-art SAR technology. The upcoming RADARSAT mission will further prove that ScanSAR is a powerful imaging technique for regional and global scale monitoring.

The Cassini Titan Radar Mapper mission, scheduled to be launched in 1997, also employs the ScanSAR operation technique [1 O]. The Cassini spacecraft will fly by Titan, the largest satellite of Saturn, 35 times in a large elliptic orbit over the planned four-year operations. During the closest approach period of each fly-by, the radar system will be alternately taking data from both sides of the flight track in the ScanSA R mode. The radar will first scan one side of the flight track for up to three beams, switch over to the other side to scan for another three beams, steer back to the original side and repeat the same sequence throughout the data acquisition. This special operation mode allows data to be acquired not only with a larger swath but also from both sides of the flight track.

A new mission is being proposed for reflying the SIR-C radar. The primary mission objective is to produce near-global scale digital topographic data sets by combining Scan SAR with interferometry. in recent years, S AR h as moved beyon d the tradi t ions] role of imaging thanks to a newly developed technique known as interferometric SAR (I FSAR) [1 1]-[1 4]. IFSAR has been proven by several airborne and satellite SAR systems, including SIR-C/X-SAR, to be a powerful alternative and mature technique for producing digital topographic maps. In

order to satisfy the immediate need for obtaining near -global scale topographic data, a new mission was conceived recently to refly the existing S1 R-C system on the space shuttle with a second C-band antenna deployed at the end of a 60-meter boom. The radar system will operate in the four-beam Scan SAR mode. With a 225-kilometer swath and 57° inclination angle, 159 orbits are all that required to cover the entire land areas within ±60° latitudes. Such a mapping process can be accomplished by an eleven-day space shuttle mission. This new mission is being vigorously pursued by NASA and the Defense Mapping Agency (DMA) for a targeted space shuttle mission in 1998. Such a quick turn-around of highly valuable topographic data sets is made possible thanks to ScanSAR.

ACKNOWLEDGMENT

The authors wish to thank the entire SIR-C project team for developing an unparalleled radar system that produce magnificent data products. Special thanks go to David Perz, Tracy Clark and Brian Swift, who modified the existing S1 R-C codes for transferring ScanSAR data, and Shirley Pang, who modified the SIR-C survey processor for processing ScanSAR data. The research described in this paper was performed at the Jet Propulsion Laboratory, California Institute of Technology, under contract with the National Aeronautics and Space Administration.

REFERENCES

[1] J. Curlander and R. McDonough, Synthetic Aperture Radar - Systems and Signal Processing, John Wiley & Sons Inc., 1991.

[2] R.J,. Jordan, " The SEA SAT - A Synthetic Aperture Radar System, " IEEE J. Oceanic Engineering, Vol. OE-5, pp. 154-163, April, 1980.

[3] W .T.K. Johnson, " Magellan Imaging Radar Mission to Venus, " Proceedings of IEEE, vol 79, no.6, pp. 777-790, June, 1991.

[4] R. Moore, J. Classen, Y.H. Lin, "Scanning Spaceborne Synthetic Aperture Radar with Integrated Radiometer, " IEEE Trans. on Aerospace and Electronics System, Vol. AES-17, No. 3, pp. 410-420, May 1981.

[5] K. Tomiyasu, "Conceptual Performance of a Satellite Borne Wide Swath Radar, " IEEE Trails. on Geoscience and Remote Sensing, Vol. GE- 19, pp. 108-116, April 1981.

[6] Special issue on SIR-C/X-SAR, IEEE Transactions on Geoscience and Remote Sensing, Vol. 33, no. 4, pp. 817-956, July 1995.

[7] R. Keith Raney, A. P. Luscombe, E.J. Langham, and S. Ahmed, "RADARSAT, " Proceedings of IEEE, vol 79, no.6, pp. 839-849, June, 1991.

[8] R.L. Jordan, B.L. Huneycutt, and M. Werner, "The SIR-C/X-SAR Synthetic Aperture Radar System, " IEEE Trans. on Geoscience and Remote Sensing, Vol. 33, no.4, pp. 829-839, July, 1995.

[9] M. Sack, M.R. Ito, I.G. Cumming, "Application of Efficient Linear FM Matched Filtering Algorithms to Synthetic Aperture Radar Processing, " IEE Proceedings, Vol. 132, Pt. F, No. 1, pp. 45-57, February, 1985.

[10] C. Elachi, E. Im, L.E. Roth, C.L. Werner, " Cassini Titan Radar Mapper, " Proceedings of IEEE, VOI 79, no.6, pp. 867-880, June, 1991.

[11] 11. Zebker and R. Goldstein, "Topographic Mapping from Interferometric SAR Observations, " Journal of Geophysical Research, Vol. 91, No. B5, pp. 4993-4999, 1986.

[12] F. Li and R. Goldstein, "Studies of Multi-Baseline Spaceborne Interferometric Synthetic Aperture Radars, " IEEE Trans. on Geoscience and Remote Sensing, Vol. 28, pp. 88-97, January 1990.

[13] 11. Zebker, ct al, "The TOPSAR Interferometric Radar q'orographic Mapping Instrument, " IEEE Trans. on Geoscience and Remote Sensing, Vol. 30, No. 5, pp. 933-940, September 1992.

[14] H. Zebker, ct al, "Accuracy of Topographic Maps Derived from ERS-1 Interferometric Radar, " IEEE Trans. on Geoscience and Remote Sensing, Vol. 32, No. 4, pp. 823-836, July 1994.

SAR Orbit	
- Nominal Altitude	215 ± 25 Km
- Eccentricity	≤ 0.002"
- Inclination	57"
Attitude Errors	
- Roll, yaw, pitch deadband	±0.1°
- Roll, yaw, pitch drift rates	±0.01°/second
Transmitter frequency	
- L-Band	1.25 GHz
- C-Band	5.30 GHz
Polarization	HH, HV, VH, W
Pulse bandwidth	10, 20, 40 MHz
Pulse duration	33.8, 16.9, 8.44 usec
Sampling rate	22.5, 45.0, 90.0 MHz
Data quantization format	4-bit, 8-bit, (8,4) BFPQ
Pulse Repetition Frequency	1344, 1395, 1440, 1488, 1512, 1620, 1674, 1736 Hz
Antenna Dimension	
- L-Band	12.1 m x 2.8 m
- C-Band	12.1 m x 0.74 m
Incidence Angles	17° to 63°

Table 1: SIR-C orbit and radar characteristics.

Flight	Datatake	Site Name	Start MET	Duration
1	32.1	North Atlantic	01/22:08:30	1 min 48 sec
	48.0	North Atlantic	02/21:51:25	1 min 15 sec
	64.0	North Atlantic	03/21 :30:30	3 min 4 sec
	101.1	Prince Albert	06/04:14:52	7 min 44 sec
	117.1	Prince Albert	07/03:55:05	7 min 48 sec
	133.1	Prince Albert	08/03:33:01	7 min 42 sec
2	32.1	North Atlantic	01/22:07:15	4 min O sec
	48.0	North Atlantic	02/21 :50:57	1 min 15 sec
	64.0	North Atlantic	03/21 :30:11	3 min 4 sec
	82.1	Chickasha	05/00:00:29	3 min 24 sec
	87.7	Weddell Sea	05/03:27:34	6 min O sec
	167.95	Weddell Sea	10/06:29:51	4 min O sec

Table 2: SIR-C ScanSAR datatakes. **Mission** Elapsed Time (MET) is in day/hour: min:sec format.

Number of Beams	4
Look Angle	30.0°, 40.5", 47.25°, 5" .0°
Radar Channels	LW, LVH, CW, CVH
PRF	1512, 1344, 1620, 1512 Hz
Data Window Position	53, 69, 51, 67 steps
Pulse Bandwidth	10 MHz
Pulse Width	33.8 micro-seconds
Dwell Time	33, 47, 34, 48 pulses

Table 3: Radar parameters for DT82.1 of the second flight.
Each DWP step is approximately 4.97 micro-seconds.

Number of Beams	**4**
Look Angle	30.0°, 40.0°, 47.5°, 51.25°
Radar Channels	LW, LVH, CW, CVH
PRF	1512, 1302, 1512, 736 Hz
Data Window Position	**65, 71, 39, 21** steps
Pulse Bandwidth	10 MHz
Pulse Width	33.8 micro-seconds
Dwell Time	34, 34, 45, 57 **pulses**

Table 4: Radar parameters for DT87.7 of the second "flight.
Each DWP step is approximately 4.97 micro-seconds.

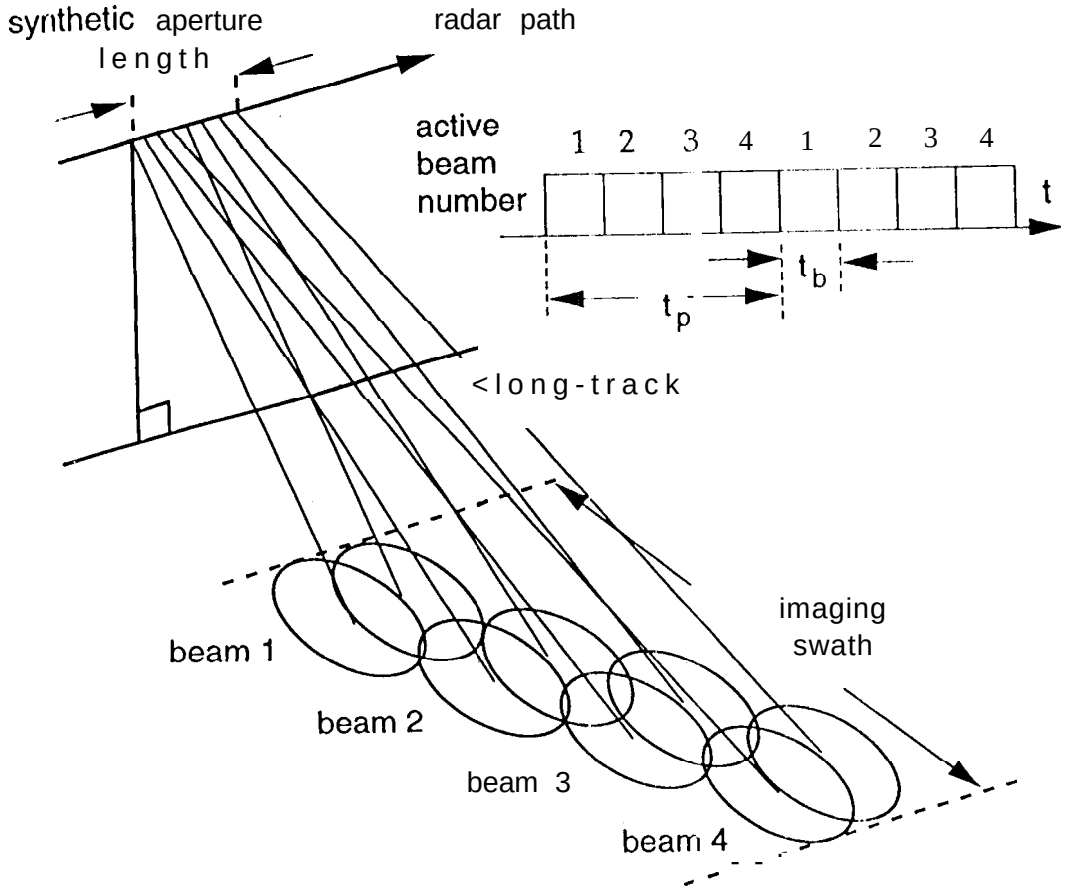

Figure 1. ScanSAR geometry and radar operation sequence

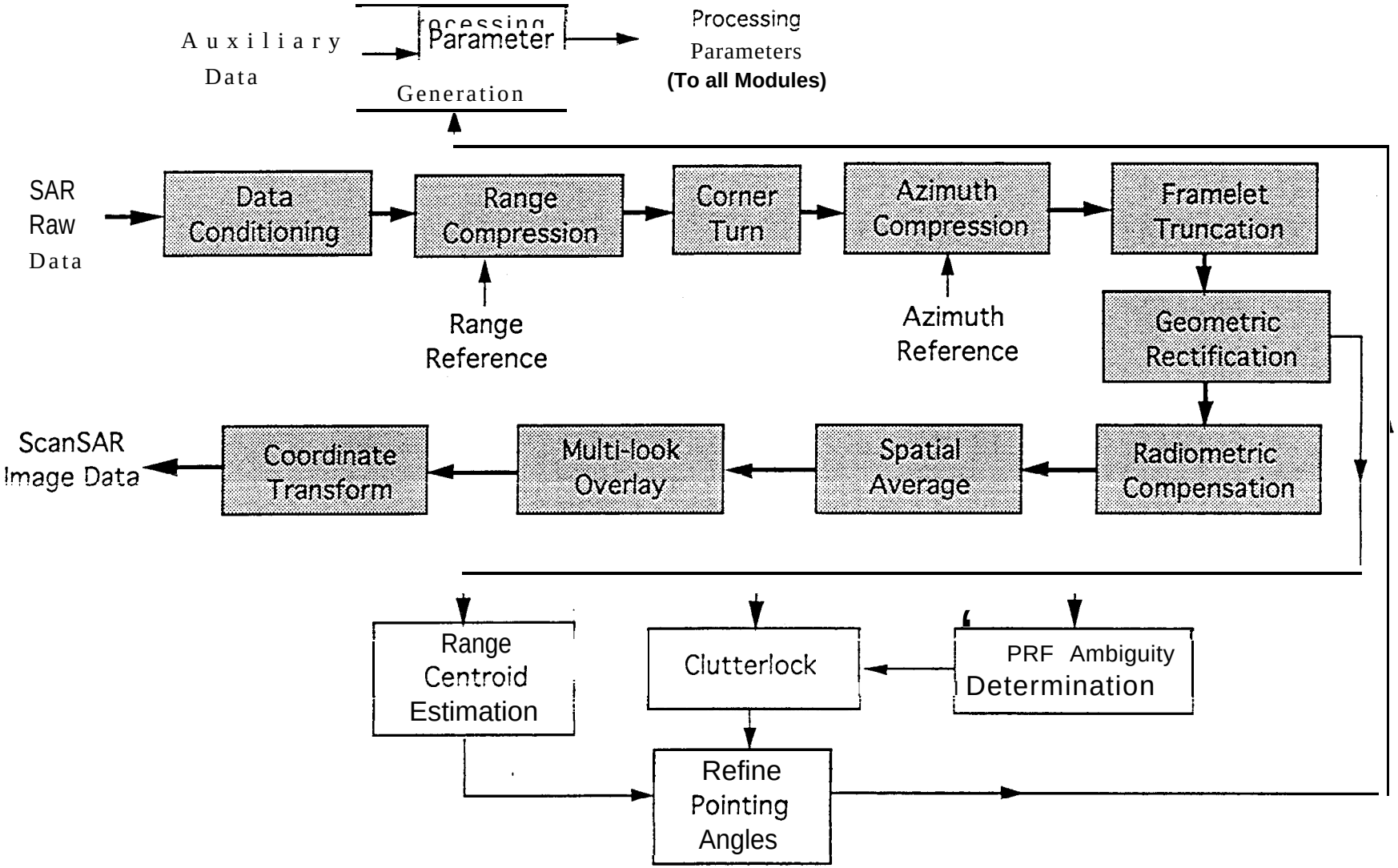

Figure 2: ScanSAR processing algorithm.

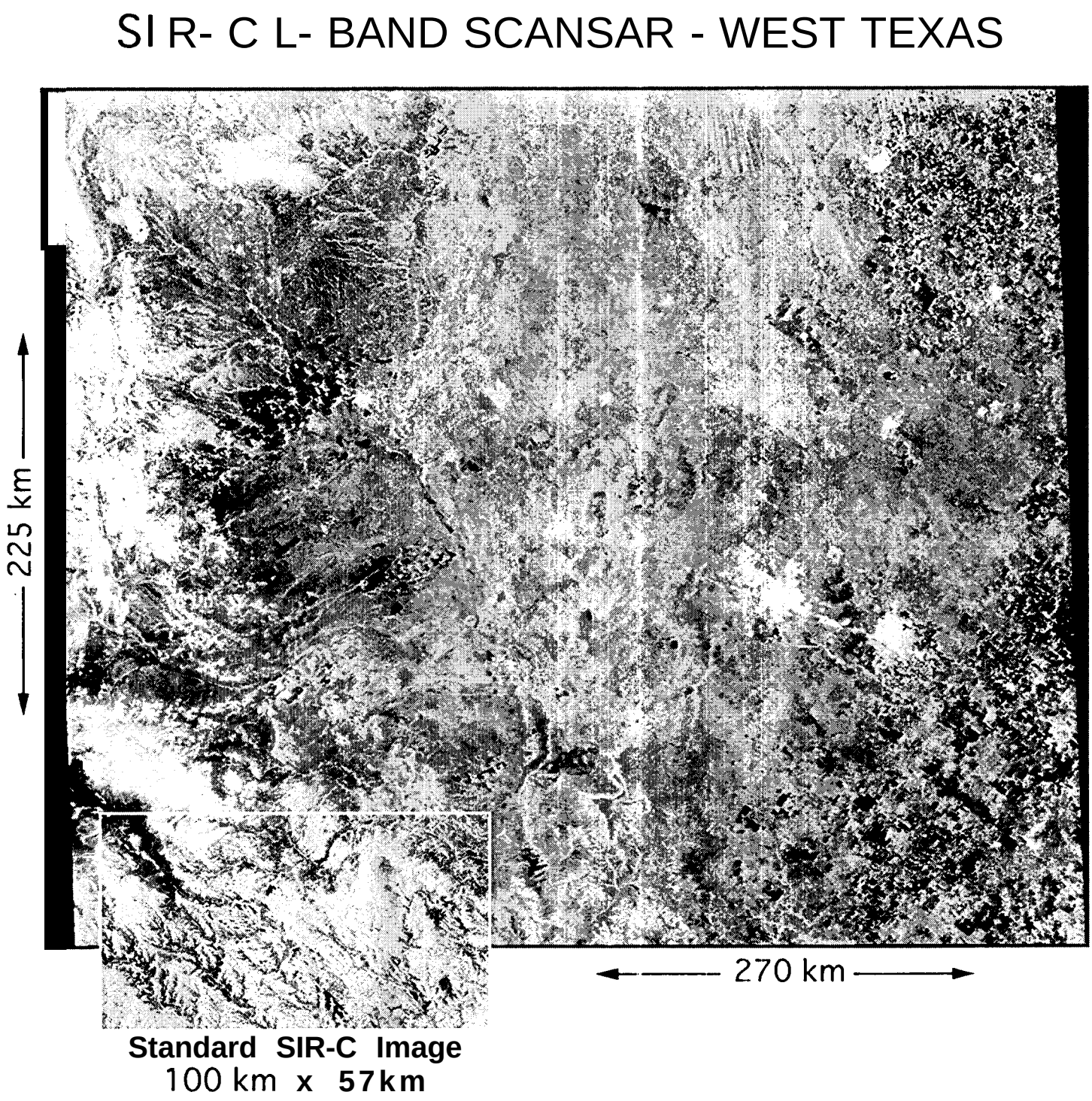

Figure 3: An example SIR-C ScanSAR image overlaid with a standard image. Data were acquired over western Texas. The radar channel is L-band, W–polarization.

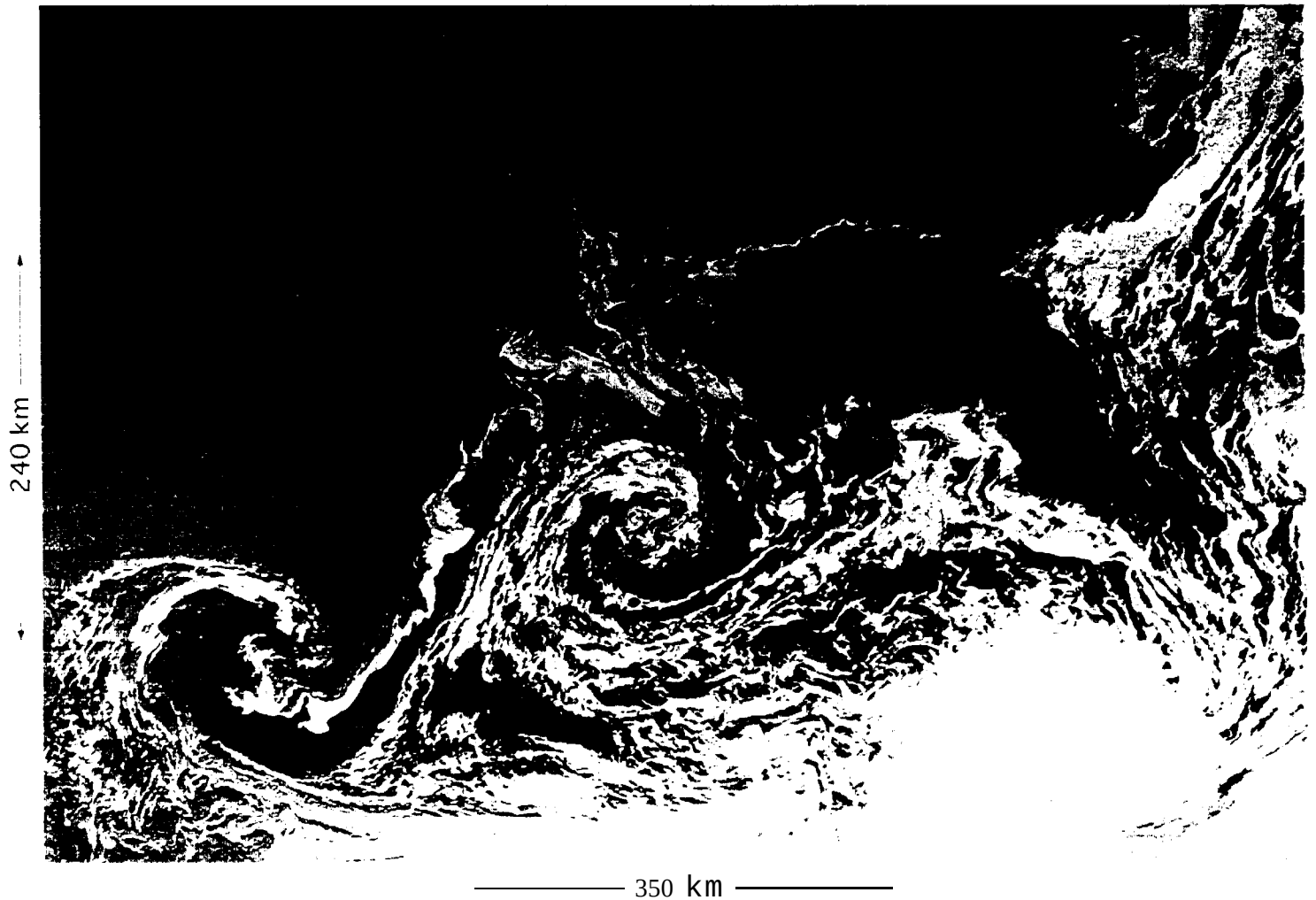

Figure 4: A color composite ScanSAR image of SIR-C. Data were acquired over the Weddell Sea, off Antarctica. The colors in this image were obtained using the following radar channels: LW is blue, LHV is green and CVV is red.